J. Synchrotron Rad. (1999). **6**, 1148–1152

First experiment by two-dimensional digital mammography with synchrotron radiation

Quanwen Yu,[a] Tohoru Takeda,[b]* Keiji Umetani,[c]† Ei Ueno,[b] Yuji Itai,[b] Yukio Hiranaka[a] and Takao Akatsuka[a]

[a]*Faculty of Engineering, Yamagata University, Yonezawa, Yamagata 992-8510, Japan,* [b]*Institute of Clinical Medicine, University of Tsukuba, Tsukuba, Ibaraki 305-8575, Japan, and* [c]*Central Research Laboratory, Hitachi Ltd, Kokubunji, Tokyo 185-8601, Japan.* *E-mail: ttakeda@igaku.md.tsukuba.ac.jp*

(*Received 20 May 1999; accepted 31 August 1999*)

Two-dimensional digital mammography with synchrotron radiation was developed to obtain high-contrast images. The system consisted of a single-crystal monochromator with an asymmetrically reflecting silicon ⟨311⟩ crystal, an avalanche multiplication-type pick-up tube camera with a fluorescent plate and lens-coupling system, and a workstation. The preliminary experiment was carried out with a synchrotron light source at the Photon Factory, KEK, in Tsukuba. Breast phantom and human breast specimen were imaged using 20 keV monochromatic synchrotron X-rays. These images were compared with images obtained by a conventional mammography system. The minimal detectable diameter of microcalcification on the breast phantom was 165 μm by the two-dimensional synchrotron radiation imaging system and 196 μm by the conventional mammography system. In the breast specimens, microcalcification and soft-tissue masses were clearly imaged and their contrasts improved by about 18% and 38%, respectively, in the two-dimensional synchrotron radiation system. The entrance surface dose of the two-dimensional synchrotron radiation system was about 400 mR, which was almost the same value as the 420 mR delivered by the conventional mammography system. Two-dimensional synchrotron radiation digital mammography is considered to be a powerful imaging modality for diagnosing breast tumors.

Keywords: monochromatic X-rays; two-dimensional digital mammography; avalanche multiplication-type pick-up tube cameras; diagnostic imaging.

1. Introduction

Mammography has been shown to be an effective technique for early detection of breast cancer (National Council on Radiation Protection and Measurement, 1986). Although the technology for mammography has advanced with the introduction of microfocus molybdenum anode X-ray tubes and high-definition screen-film systems, it is well known that nodules less than 2–3 mm in size are difficult to detect by mammography with conventional X-ray sources. The molybdenum anode X-ray tubes are operated at 25–30 kVP, and the obtained spectrum consists of two peak fluorescent lines ($K_{\alpha1}$ = 17.4 keV, $K_{\alpha2}$ = 19.6 keV) superimposed on a continuous spectrum. They do not have sufficient intensity for Bragg diffraction to provide monochromatic beams with an adequate photon flux. Generally, the difference in absorption coefficients between cancer and normal tissues increases at photon energies of less than 20 keV. However, conventional mammography does not demonstrate this difference because it uses photon energies of more than 20 keV. In addition, X-rays with a photon energy of more than 20 keV produce significant Compton scattering from objects, which serves only to diminish the image contrast.

Synchrotron radiation has excellent properties such as high X-ray flux, continuous spectrum and small divergence. High X-ray flux and continuous spectrum allow the use of a crystal monochromator to select the most suitable energy for mammography. Small divergence of synchrotron X-rays permits a long object-to-detector distance for the imaging and reduces the superimposed scattering radiation from objects. In conventional mammography the finite source size will cause loss of spatial resolution by geometrical magnification, whereas the influence of the synchrotron radiation's source size on spatial resolution is very small because of the small divergence of the X-ray beam. Therefore, the use of a monochromatic X-ray beam is ideal for obtaining mammographic images with significantly enhanced contrast and high resolution for the early detection of small breast nodules.

Monochromatic synchrotron radiation mammography with a line scan mode using a fan-shaped X-ray beam has

† Present address: Japan Synchrotron Radiation Research Institute (JASRI), SPring-8, Sayo-gun, Hyogo 697-5198, Japan.

been employed in Italy (Arfelli *et al.*, 1995, 1998; Burattini *et al.*, 1992, 1995), the USA (Johnston *et al.*, 1995, 1996) and the UK (Lewis *et al.*, 1999). Using a linear array silicon pixel detector, an imaging plate and conventional mammographic film, high-contrast images of breast phantom and breast tissue were obtained with similar or less radiation doses than that of conventional X-ray images. In Japan, two-dimensional synchrotron radiation mammograms of breast phantom were obtained and small microcalcifications which were not revealed by conventional mammography are clearly detected at 20 keV energy (Umetani *et al.*, 1998). The advantage of the two-dimensional system is easy acquisition of large objects similar to conventional mammography without mechanical scanning apparatus. Moreover, we can easily apply stereoscopic imaging of breast tumors. In this preliminary study, using the two-dimensional synchrotron radiation digital mammographic system, details of experimental results for human breast specimens and breast phantoms are discussed and compared with conventional mammography.

2. Materials and methods

2.1. *Two-dimensional synchrotron radiation digital mammographic system*

The two-dimensional synchrotron radiation digital mammographic system was constructed with the superconducting vertical wiggler (5 T) beamline BL-14C at the Photon Factory in Tsukuba. This system consisted of a single-crystal monochromator with an asymmetrically reflecting silicon ⟨311⟩ crystal, an object table, a fluorescent plate (HR-4, Fuji Medical Systems Co. Ltd), an avalanche multiplication-type pick-up tube camera (Hitachi Ltd), a coupling lens system between the fluorescent plate and the camera, an image-acquisition system and a workstation (Fig. 1). A 35 mm × 7 mm white X-ray beam from a storage ring was monochromated and expanded 3.5 times in the horizontal direction by the asymmetric reflection on the silicon crystal planes to a 35 mm × 25 mm monochromatic X-ray beam. The X-ray energy was adjusted to 20 keV. One image was acquired in 66.7 ms. The distance between the object and sensor was maintained at about 5 cm to reduce overlap of scattered X-rays from the object. The storage ring was operated at 2.5 GeV with an average current of 300 mA. In front of the object, the incident monochromated flux was $\sim 9 \times 10^8$ photons mm^{-2} s^{-1}.

The avalanche multiplication-type pick-up tube camera was used to obtain better spatial resolution and better dynamic range of the X-ray image (Umetani *et al.*, 1996). The high-sensitivity camera was 32 times more sensitive to incident light photons than the conventional pick-up tube cameras and also had a wide dynamic range (∼1000:1) (Takeda *et al.*, 1997).

In this system the X-ray images were converted to light images by the fluorescent plate and these optical images were focused on the photoconductive layer of the pick-up tube using a coupling lens with high numerical aperture. The viewing field was 50 mm × 50 mm on the fluorescent plate and X-ray images were digitized into a 1024 × 980 matrix by a 12-bit analog-to-digital converter, so the pixel size corresponded to about 50 µm. However, the actual resolution was about 60 µm due to resolution limitations of the fluorescent screen at the monochromatic X-ray energy of 20 keV (Umetani *et al.*, 1998). The workstation was used for image processing and controlling the image-acquisition system.

2.2. *Image processing operations*

To obtain the precise digital images a set of three images was acquired: an image without X-ray exposure (dark-current image), an X-ray image without an object (X-ray source image) and an object image. The dark-current component of the camera's output was removed by subtracting the dark-current image from the object image and X-ray source image. Correction of non-uniformity of the X-ray source and detection system was performed by dividing the object image by the X-ray source image.

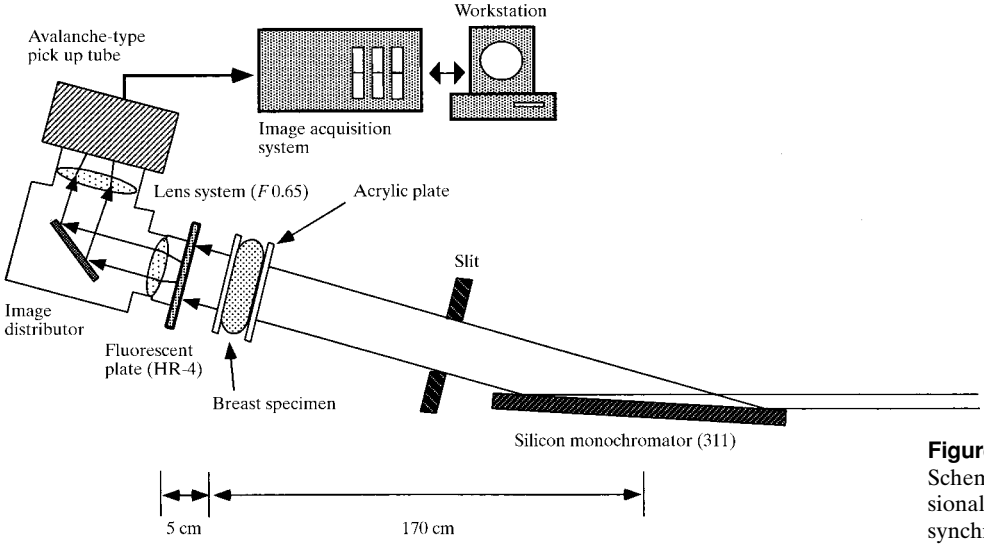

Figure 1
Schematic diagram of the two-dimensional digital mammographic system with synchrotron radiation.

As the beam size in this system was limited to 35 mm × 25 mm, a whole breast specimen could not be imaged simultaneously. Therefore, to obtain an image of a whole breast specimen, image connection of six radiograms was performed using landmarked structures on images such as calcified lesion and fibrosis of breast tissue.

2.3. *Objects*

The experimental objects were a standard breast phantom (Model 11A, CIRS, Inc., Virginia) and human breast specimen. The phantom was 4.5 cm thick, and consisted of microcalcifications, masses, fibrils and line-pair test targets. The breast specimen was surgically prepared and included cancer nodules.

To compare the results with those of the conventional X-ray source, the same standard mammographic phantom and breast specimen were also imaged with the conventional mammographic system (Mammomat 3000, Siemens). Images were obtained at 27 kVP with 32 mA using Mo filters with an antiscattering grid (grid radio 5:1). The films were digitized by the Drum Scanner (Densitometer 2605 Abe-Sekkei Ltd, Tokyo) at a pixel size of 50 μm × 50 μm and 12-bit grey levels.

2.4. *Definition of image contrast*

Image contrast I_c on a mammogram (Arfelli *et al.*, 1998; Johnston *et al.*, 1995) was defined by the following equation,

$$I_c = (I_1 - I_0)/I_0, \tag{1}$$

where I_1 is the average intensity of the measured signal of target objects such as a soft-tissue mass and calcification and I_0 is the average intensity of the surrounding region. Ten regions of calcification and soft-tissue tumors were measured.

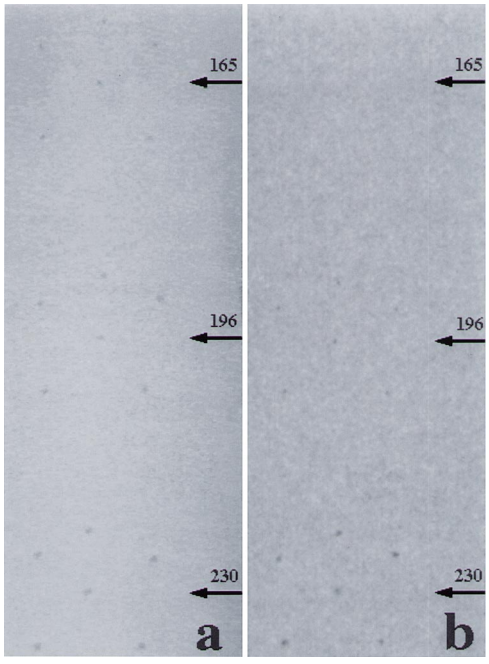

Figure 2
Mammogram of breast phantom. (*a*) Two-dimensional synchrotron radiation image. (*b*) Conventional mammographic image.

2.5. *Dose evaluation*

Concerning synchrotron radiation images, the entrance surface dose was measured using a thermoluminescent dosimeter (TLD). TLD chips were placed at the object position after object imaging. For comparison, the entrance surface dose from conventional mammography was also measured by using the ion chamber dosimeter.

3. Results

Images of the standard breast phantom were obtained both by the two-dimensional synchrotron radiation digital mammographic system (Fig. 2*a*) and the conventional mammographic system (Fig. 2*b*). Two-dimensional synchrotron radiation digital mammography detected microcalcification of 165 μm in diameter. This size of microcalcification was not imaged by conventional mammography, the detectable diameter of which was 196 μm.

The human breast specimen was also imaged by the two-dimensional synchrotron radiation mammographic system (Fig. 3*a*) and conventional mammographic system (Fig. 3*b*). Two-dimensional synchrotron radiation mammography imaged more clearly the calcified lesion and the soft-tissue mass compared with conventional mammography. Good differentiation was obtained among breast tumor lesions, fibrous tissue and surrounding adipose tissue.

The image contrast was measured in the breast specimen. The image contrast of microcalcification and the soft-tissue mass was improved by about 18% and 38%, respectively, in the synchrotron radiation image system (Table 1).

The entrance surface doses of the synchrotron radiation system and conventional mammography were about 400 mR and 420 mR, respectively. Therefore, the entrance surface dose delivered by a 20 keV monochromatic beam was almost the same as that delivered by the conventional mammographic system.

4. Discussion

4.1. *Imaging of two-dimensional digital mammography*

In this preliminary experiment synchrotron radiation mammograms were obtained two-dimensionally using the video camera and fluorescent plate system with an area-shaped X-ray beam produced by asymmetric reflection of a crystal monochromator. The entrance surface dose delivered by the 20 keV monochromatic synchrotron X-ray was almost the same as that delivered by the conventional mammographic system. However, significant improvement of image contrast was obtained by two-dimensional synchrotron radiation mammography. Two-dimensional synchrotron radiation mammography clearly imaged microcalcifications within breast cancer and the tumor

Table 1
Percentage of improvement of image contrast measured for the breast specimen.

	Image contrast		
	Two-dimensional SR mammography	Conventional mammography	Improvement
Calcification	57.7 ± 10.7	40.2 ± 10.2	17.7 ± 1.5
Soft tissue	47.2 ± 6.5	9.5 ± 4.7	37.9 ± 4.7

margin was precisely detected. Quantitative analysis showed that the image contrast improved by about 18% in calcified lesions and 38% in soft-tissue masses compared with conventional mammography.

This improvement of image contrast by two-dimensional synchrotron radiation mammography was due to several properties of synchrotron radiation such as monochromatic X-rays with high flux and small beam divergence which allows reduction of the amount of superimposed scattering component from the object by placing the two-dimensional detector away from the object. X-ray statistical noise in the synchrotron radiation system is comparable with the conventional mammography system because the entrance surface dose delivered by a 20 keV monochromatic beam was almost the same as that by the conventional mammography system. For this reason the factors that affect the image quality are the use of monochromatic X-rays and the removal of the scattered radiation. Computer simulation (Boone & Seibert, 1994) showed that monochromatic X-rays exhibited 40–200% improvement in tissue contrast when imaging the chest with different contrast targets such as soft tissue and calcified lesions. Furthermore, qualitative study with synchrotron radiation mammography using phantom and specimens showed that higher contrast and better resolution were obtained with similar or reduced radiation doses compared with conventional mammography (Burattini *et al.*, 1992, 1995). Another study of the breast phantom revealed that images obtained with synchrotron radiation at 20 keV showed about 18% contrast improvement (Johnston *et al.*, 1995). In our preliminary experiment the image contrast improved by about 18% in calcified lesions and 38% in masses of soft tissue compared with conventional mammography. Significant improvement of soft-tissue contrast may be caused by reduction of superimposed scattering X-rays from an object due to an air gap.

In addition, digital mammography has numerous potential advantages over screen-film mammography (Roehrig *et al.*, 1993; Feig & Yaffe, 1998). It has a wider dynamic range (the linear response may be 1000:1 compared with 40:1 for screen-film mammography), so the greater contrast resolution can be obtained, especially in dense breast tissue. In digital mammography it is easy to adjust the image with optimal brightness and contrast for observation.

4.2. *Present problems and future improvements*

Our view field was limited to 35 mm × 25 mm because the asymmetrically reflecting silicon ⟨311⟩ crystal monochromator was prepared for angiography at an energy of 33.2 keV and not for mammography at an energy of 20 keV (Umetani *et al.*, 1996). A larger field of view can be easily obtained by manufacturing an asymmetrically cut crystal suitable for mammography.

Spatial resolution was about 60 μm for our HR-4 fluorescent screen. If the HR-3 fluorescent screen is applied, a spatial resolution of 50 μm would be obtained by 20% higher resolution.

Further reduction of scatter contamination from objects may markedly improve the image contrast. In conventional mammography the air-gap technique is not applicable because of large geometrical magnification caused by the long object-to-detector distance. In the large geometrical magnification, isotropic emission in space requires a large detector and the finite source size will cause the loss of

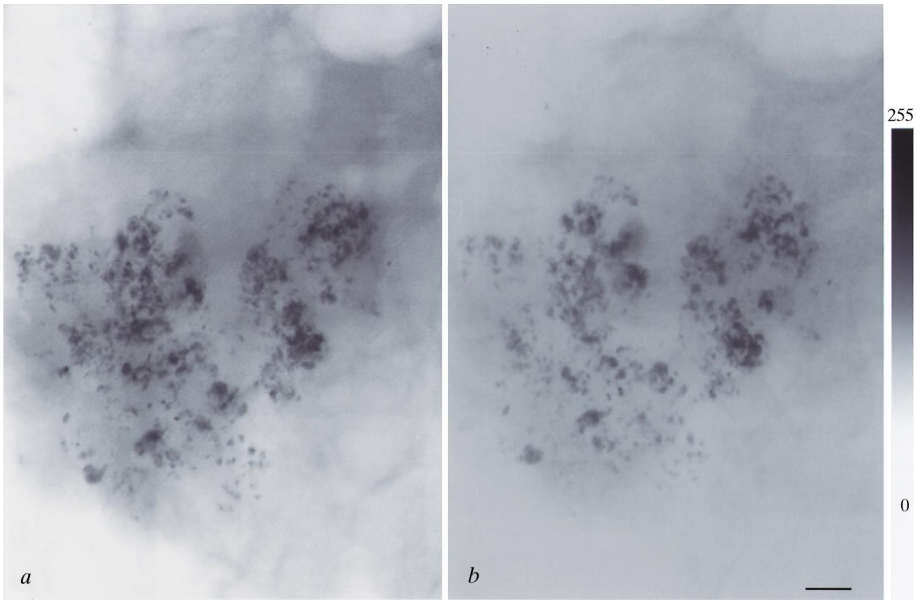

Figure 3
Mammogram of human pathological specimen. (*a*) Two-dimensional synchrotron radiation image. (*b*) Conventional mammographic image. Scale bar: 5 mm.

spatial resolution. However, the synchrotron radiation X-ray beam has a small beam divergence, so the air-gap technique can be easily used.

The horizontal and vertical source sizes of the superconducting vertical wiggler beamline BL-14C are 1.05 and 0.096 mm, respectively. The experimental hutch is located at about 40 m from the source. The effect of source spot size on spatial resolution of the image is expressed as follows,

$$u = l(b/a), \tag{2}$$

where u is the broadening width of the spot size, l is the size of the source, a is a distance from the source to the object and b is the distance from object to detector (air gap). In this experimental set-up, a is 40 m and the air gap b is 5 cm. The values of u are less than 1 μm in both the horizontal and vertical directions and are negligibly small. The use of a suitable experimental set-up allows the air-gap technique to be applied more effectively and higher-quality images than the present images can be obtained by perfect scattered X-ray removal using the very large air gap.

The optimal energy for mammography is known to be in the range 17–21 keV and to depend on breast thickness (Jennings *et al.*, 1981; Motz & Danos, 1978; Ragozzino, 1982). In our experiment a monochromatic X-ray beam of 20 keV was selected for imaging. Using an X-ray energy of 18.2 keV, the image contrast was expected to improve by 25%, but the X-ray dose for patients will increase by 1.7 times compared with that at an X-ray energy of 20 keV (Burattini *et al.*, 1992; Johnston *et al.*, 1995). Even with a 20 keV X-ray energy image, use of the air gap will improve the image contrast, so we can use this energy with a significantly lower X-ray dose.

5. Conclusions

Two-dimensional synchrotron radiation digital mammography was developed with high contrast and slightly high spatial resolution. The preliminary experiment demonstrated it could detect microcalcifications and masses of soft tissue in breast specimens more clearly than the conventional mammographic system under the same radiation dose. Thus, we can conclude that the use of two-dimensional synchrotron radiation digital mammography may result in earlier detection of breast tumors.

The authors thank Kazuyuki Hyodo PhD of the Photon Factory for his support in experiments at BL-14C, and Teruo Watanabe MD, PhD for his support with the pathological specimen, Noboru Chiba RT, Hiroshi Yokota RT, Toshihiro Kusumoto RT and Mr Tatsuo Ito for their technical help, Mr Kouzou Kobayashi for his technical support of this experimental apparatus, and Mrs Yukiko Kawata for her help preparing this paper. Experiments were performed under proposal number #97G162 approved by the High Energy Accelerator Research Organization. A part of this study was presented at JAMIT 98 held in Tokyo in July 1998 (Yu *et al.*, 1998).

References

Arfelli, F., Bonvicini, V., Bravin, A., Cantatore, G., Castelli, E., Palma, L., Di Michiel, M., Longo, R., Olivo, A., Pani, S., Pontoni, M., Poropat, P., Prest, M., Rashevsky, G., Tromba, G. & Vacchi, A. (1998). *Radiology*, **208**, 709–715.

Arfelli, F., Bravin, A., Barbiellini, G., Cantatore, G., Castelli, E., Di Michiel, M., Poropat, P., Dalla Palma, L., Longo, R., Bernstorff, S., Savoia, A. & Tromba, G. (1995). *Rev. Sci. Instrum.* **66**, 1325–1328.

Boone, J. M. & Seibert, J. A. (1994). *Med. Phys.* **21**, 1853–1863.

Burattini, E., Cossu, E., Di Maggio, C., Gambaccini, M., Indovina, P. L., Marziani, M., Pocek, M., Simooni, S. & Simonetti, A. T. G. (1995). *Radiology*, **195**, 239–244.

Burattini, E., Gambaccini, M., Marziani, M., Rimondi, O., Indovina, P. L., Pocek, M., Simonetti, G., Benassi, M., Tirelli, C. & Passariello, R. (1992). *Rev. Sci. Instrum.* **63**, 638–640.

Feig, S. A. & Yaffe, M. J. (1998). *Radiographics*, **18**, 893–900.

Jennings, R. J., Eastgate, R. J., Siedband, M. P. & Ergun, D. L. (1981). *Med. Phys.* **18**, 629–639.

Johnston, R. E., Washburn, D., Pisano, E., Burns, C., Thomlinson, W. C., Chapman, L. D., Arfelli, F., Gmur, N. F., Zhong, Z. & Sayers, D. (1996). *Radiology*, **200**, 659–663.

Johnston, R. E., Washburn, D., Pisano, E., Thomlinson, W. C., Chapman, L. D., Gmur, N. F., Zhong, Z. & Sayers, D. (1995). *Proc. SPIE*, **2432**, 434–441.

Lewis, R. A., Hufton, A. P., Hall, C. J., Helsby, W. I., Towns-Andrews, E., Slawson, S. & Boggis, C. R. M. (1999). S*ynchrotron Rad. News*, **12**, 7–14.

Motz, J. W. & Danos, M. (1978). *Med. Phys.* **5**, 8–22.

National Council on Radiation Protection and Measurement (1986). NCRP Report No. 85, pp. 1–82. Bethesda, USA.

Ragozzino, M. W. (1982). *Med. Phys.* **9**, 493–496.

Roehrig, H., Fajardo, L. & Yu, T. (1993). *Proc. SPIE*, **1896**, 213–224.

Takeda, T., Umetani, K., Doi, T., Echigo, J., Ueki, H., Ueda, K. & Itai, Y. (1997). *Acad. Radiol.* **4**, 438–445.

Umetani, K., Ueki, H., Takeda, T., Itai, Y., Akisada, M. & Sasaki, Y. (1998). *Medical Applications of Synchrotron Radiation*, edited by M. Ando & C. Uyama, pp. 83–86. Tokyo: Springer Verlag.

Umetani, K., Ueki, H., Ueda, K., Hirai, T., Takeda, T., Doi, T., Wu, J., Itai, Y. & Akisada, M. (1996). *J. Synchrotron Rad.* **3**, 136–144.

Yu, Q., Takeda, T., Umetani, K., Uchida, A., Yuasa, T., Itai, Y. & Akatsuka, T. (1998). *Med. Imag. Tech.* **17**, 437–438.